

Characterization of a Multimodal and Multispectral Led Imager: Application to Organic Polymer's Microspheres with Diameter $\Phi = 10.2 \mu\text{m}$

Marcel A. Agnero^{1,2}, Jérémie T. Zoueu¹, Kouakou Konan¹

¹Laboratoire d'Instrumentation d'Image et Spectroscopie, Institut National Polytechnique Félix Houphouët-Boigny, Yamoussoukro, Côte d'Ivoire

²Laboratoire de Physique de la Matière Condensée et Technologie, University Félix Houphouët-Boigny, Abidjan, Côte d'Ivoire

Email: jeremie.zoueu@inphb.edu.ci

Received 25 May 2016; accepted 18 July 2016; published 21 July 2016

Copyright © 2016 by authors and Scientific Research Publishing Inc.

This work is licensed under the Creative Commons Attribution International License (CC BY).

<http://creativecommons.org/licenses/by/4.0/>



Open Access

Abstract

Multispectral microscopy enables information enhancement in the study of specimens because of the large spectral band used in this technique. A low cost multimode multispectral microscope using a camera and a set of quasi-monochromatic Light Emitting Diodes (LEDs) ranging from ultraviolet to near-infrared wavelengths as illumination sources was constructed. But the use of a large spectral band provided by non-monochromatic sources induces variation of focal plan of the imager due to chromatic aberration which rises up the diffraction effects and blurs the images causing shadow around them. It results in discrepancies between standard spectra and extracted spectra with microscope. So we need to calibrate that instrument to be a standard one. We proceed with two types of images comparison to choose the reference wavelength for image acquisition where diffraction effect is more reduced. At each wavelength chosen as a reference, one image is well contrasted. First, we compare the thirteen well contrasted images to identify that presenting more reduced shadow. In second time, we determine the mean of the shadow size over the images from each set. The correction of the discrepancies required measurements on filters using a standard spectrometer and the microscope in transmission mode and reflection mode. To evaluate the capacity of our device to transmit information in frequency domain, its modulation transfer function is evaluated. Multivariate analysis is used to test its capacity to recognize properties of well-known sample. The wavelength 700 nm was chosen to be the reference for the image acquisition, because at this wavelength the images are well contrasted. The measurement made on the filters suggested correction coefficients in transmission mode and reflection mode. The experimental instrument recognized the microsphere's properties and led to the extraction of the standard transmittance and reflectance spectra. Therefore, this microscope is used as a conven-

tional instrument.

Keywords

Multispectral Imaging, Reference Wavelength, Correction Coefficients, Modulation Transfer Function

1. Introduction

Multispectral microscopy establishes a link between spatial and spectral information resulting from light-matter interaction. It can be described as spectroscopy and microscopy coupler. This technique is well established in remote sensing and satellite imagery areas. It is now extended to the microscopy area because of its various advantages.

Several works illustrate the importance of multispectral microscopy. Zoueu *et al.* [1] have shown that using multispectral imaging allows detecting malaria without using fluorescent labels for parasites as it is the case of thick and thin blood smears. Multispectral imaging is an important tool in the delimitation of reserved forests [2] and also in agriculture framework for rapid detection of fruit diseases [3] [4].

Several multispectral imaging technologies, in spite of their high cost, are used in the sequential or parallel acquisition of images of the same scene using different wavelengths and generate an optical spectrum associated to any pixel in the image [5]. Progresses are observed in the implementation of low cost multi spectral imaging devices. Merdasa *et al.* [6] have modified a classical microscope where the white source is replaced by quasi monochromatic sources and adapted to multispectral imaging device to detect malaria. But the microscope is limited to five spectral channels (wavelengths) in the visible spectral range. Increasing the number of spectral channels in the visible spectrum and expanding channel acquisition to the light that is outside the sensitivity of the human eye offer several advantages. Mikkel Brydegaard *et al.* [2] have constructed a multispectral microscope with a large spectral band ranging from ultraviolet to near-infrared wavelengths, active in transmission mode and which allows an information enhancement in the study of specimen.

In such a system, the spectral information reconstruction requires images of acceptable quality (sharp and of the same scale). But, using a large spectral band induces the variation of focal plan position of the imager due to the phenomenon of chromatic aberration which affects the quality of the images. This is a major problem met in multispectral imaging. To reduce distortion due to chromatic aberration, reflex objective can be used such as Cassgrain objective [7]; a two-lens system or an apochromatic triplet equips some systems to reduce curvature of the image and to minimize residual aberrations in the focal plane [8] [9]. The method of refocusing focal plan of the multispectral device can be done at each spectral channel [10]. This solution can introduce a geometrical offset on one hand and slow down the acquisition protocol of the imaging system on the other hand.

In the present work, a low cost multimode multispectral microscope with Cassgrain objective using a camera and a set of monochromatic Light Emitting Diodes (LEDs) as illumination sources was constructed and we present a new approach to calibrate that instrument to be a standard one. By calibration, we mean:

- the determination of the wavelength used to fix its focal plan where the phenomenon of chromatic aberration is more reduced,
- the correction of the extracted spectra from the images making them in agreement with the standards spectra,
- the determination of modulation transfer function which is an important tool in an imager's characterization,
- the evaluation of its capacity to recognize the specimen's properties.

For this purpose, we used it to make measurements on samples with well-known properties such as homogeneous filters and organic polymer's microspheres (latex) with diameter $\Phi = 10.2 \mu\text{m}$ before using it on specimen with unknown properties. Measurements were done in transmission mode, reflection mode and scattering mode. Results are analyzed using multivariate analysis methods.

2. Materials and Methods

2.1. Multi Spectral Device's Description

Figure 1 presents the multimodal and multispectral microscope constructed. The device used in this work is an

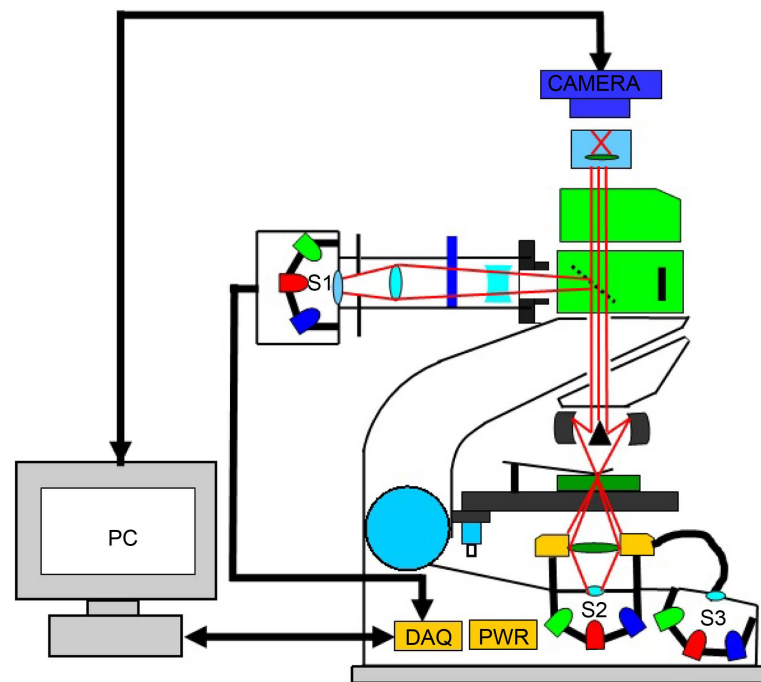


Figure 1. Multimodal and multispectral microscope setup. S1, S2 and S3 are a set of LED light sources for reflection, transmission and scattering modes respectively. The red lines illustrate the beam path interacting with the specimen.

improved version of the LED multispectral microscope built by Brydegaard *et al.* [2], adapted and described by Zoueu *et al.* [7].

The light sources S1, S2 and S3 are controlled via a data acquisition (DAQ) connected to a computer (PC). All are controlled by a LabView (Lab View 8.6, licence no. M 74 × 11278) operation code. Each light source is a set of quasi-monochromatic Light Emitting Diodes (LEDs) with the following spectral band: 375 nm, 400 nm, 435 nm, 470 nm, 525 nm, 590 nm, 625 nm, 660 nm, 700 nm, 750 nm, 810 nm, 850 nm, 940 nm. Before any measurement, we need to align all the optics. All the measurements are done in the darkness to minimize background light.

2.2. Measurement's Procedure

Measurements are made on two types of samples:

- Filters, used as homogeneous samples whose standard spectra are extracted from the spectrometer (Compact Spectra Suite Ocean Optics USB4000).

- Organic polymer's microspheres (latex) with diameter $\Phi = 10.2 \mu\text{m}$ whose properties are known. There are the homogeneity, the isotropicity and the spherical geometry.

The microspheres' samples are prepared on slides made of the highest purity, corrosion-resistant glass with dimensions $75 \text{ mm} \times 25 \text{ mm} \times 1 \text{ mm}$. The measure in each mode (transmission, reflection or scattering) needs three types of images acquired in the same acquisition conditions:

- The image T_s , R_s or S_s if it's about transmittance's measure, reflectance's measure or scattering's measure respectively. That image contains noise due to the parasite light in the dark environment and to the set-up electronic system;

- The image T_d , R_d or S_d is due to noise respectively in transmission mode, reflection mode or scattering mode;

- The image T_b , R_b or S_b is for the reference in transmission mode, reflection modes or scattering mode respectively.

To make the measurement, we first select a wavelength of illumination called reference wavelength. One illuminates the sample at this wavelength and we make sure that the image is well contrasted before running the

measurement. The measurement is an automated acquisition of thirteen images from the same scene and each image corresponds to a wavelength of illumination. The wavelengths selection as reference is part of the goals of this study.

In the transmission mode, we active the geometry “brightfield” as indicated on the interface presented by Lab view operation code. The signal T_s is measured after having put the slide containing the sample on the microscope’s holder. The reference signal T_b in the transmission mode is measured by maintaining the same slide on the microscope’s holder so that an image of the around area of the sample is acquired. For the measure of T_d , the microscope’s holder is kept empty and the electric battery for the different LEDs is set off to avoid eventual illumination of the camera. In order to rise up the acquisition speed, we establish a measurement protocol, that’s to say we acquire one of the signals T_s , T_b or T_d in a specific condition; this condition constitutes the protocol we call through our operation code to acquire the two other signals.

The corrected image T of the sample is given by the relation (1):

$$T = \frac{T_s - T_d}{T_b - T_d}. \quad (1)$$

In the measurement of the reflectance, the alignment of optics in the microscope and fixation of its focal plan at the reference wavelength being done during the measures in transmission mode, we active the geometry “reflection” in the Lab view code interface in order to run the automated acquisition of the thirteen images. The signal R_s is measured after having put the slide containing the sample on the microscope’s holder. The signal R_b is acquired by using a diffuser in the place of the sample, with its white face up in the microscope. The diffuser eliminates dissymetry light dispatching and allows a uniform intensity distribution in the camera’s field of view [3]. To acquire the image, R_d , the microscope’s holder is kept empty in order to get parasite reflection due to the optics in the microscope. The corrected image R of the sample is given by the relation (2) [3]:

$$R = \frac{R_s - R_d}{R_b - R_d}. \quad (2)$$

In scattering mode, the geometry “darkfield” is activated to run the automated acquisition of the thirteen images. The signal S_s is measured after having put the slide containing the sample on the microscope’s holder. The signal S_b is measured by using a diffuser in the place of the sample, with its white face down in the microscope. To get the image S_d , we put an empty slide on the microscope’s holder. The corrected image S of the sample is given by the relation (3):

$$S = \frac{S_s - S_d}{S_b - S_d}. \quad (3)$$

3. Results and Discussion

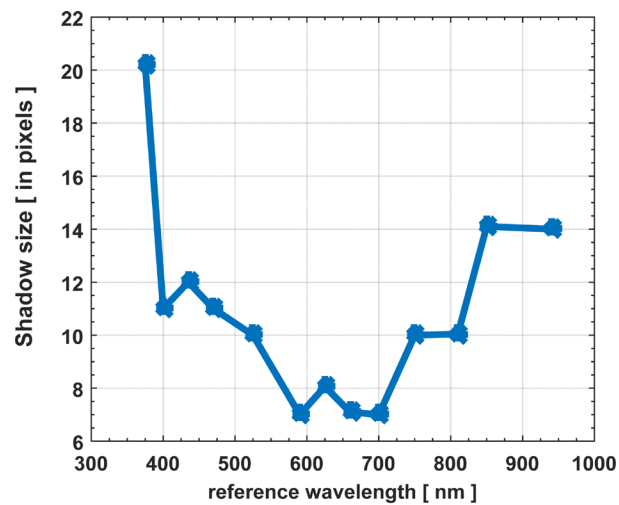
3.1. Choice of Reference Wavelength

The measure on a specimen in a mode consists to run an automated acquisition of a set of thirteen images from the same scene with each image corresponding to one wavelength of illumination. But before running the automated acquisition, we choose a wavelength of illumination called reference wavelength. We illuminate the sample at this wavelength and we appreciate the contrast of the image before doing the measurement. The contrast of the image reveals that the image is in the focal plan (of the multi spectral microscope) corresponding to that reference wavelength. But, the focal plan of an optical system depends on the wavelength of illumination (light) which passes through the system. Since the acquisition is made on a set of the thirteen quasi-monochromatic sources, then the other twelve images are not in focal plan defined by the chosen reference wavelength. This constitutes a difficulty in a multi spectral imaging system using a large spectral band. The variation of focal plan position is due to the phenomenon of chromatic aberration depending on the refractive index variation of the optical system in function of the wavelength for the light passing through it. This phenomenon rises up the diffraction effects and blurs the images inducing shadow around them. To get the best reference wavelength for all the three modes, we used each of the thirteen wavelengths as a reference wavelength followed by the acquisition of the set of the thirteen images in transmission mode. Then, we proceed with two types of images compar-

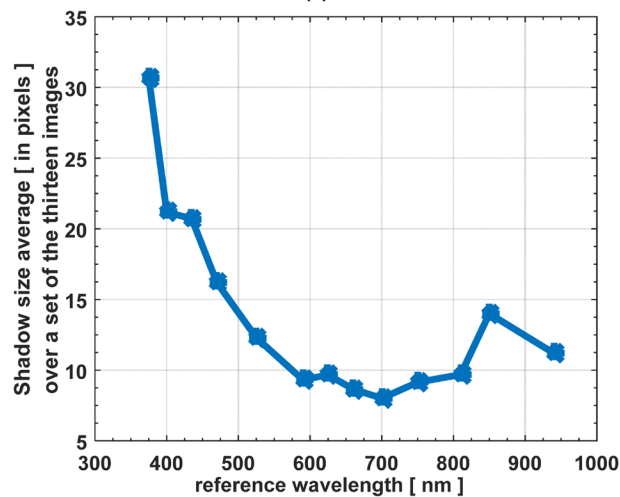
ison. Each wavelength chosen as a reference defines a focal plan. In each set of the thirteen images acquired after the choice of the reference, there's only one image which is well contrasted. Indeed, this image is acquired with light source used to fix the focal plan. Then, we have thirteen contrasted images, each one corresponding to a reference wavelength. First, we compare these thirteen contrasted images to appreciate that presenting more reduced shadow. This comparison highlights that the reference wavelengths 590 nm, 625 nm, 660 nm and 700 nm are the ones whose corresponding images present more reduced shadow spreading on 7 pixels, 8,06 pixels, 7,07 pixels and 7 pixels respectively (**Figure 2(a)**). In second time, we determine the mean of the shadow size over the images from each set. The comparison shows in **Figure 2(b)** that the reference wavelengths 590 nm, 625 nm, 660 nm, 700 nm and 750 nm are the ones whose corresponding set of images present more reduced shadow spreading on 9.31 pixels, 9.67 pixels, 8.66 pixels, 8.01 pixels and 9.14 pixels respectively.

The first comparison shows that fixing the focal plan with the reference 590 nm or 700 nm, the microsphere's image observed at the wavelength 590 nm or 700 nm respectively, present more reduced shadow (**Figure 2(a)**).

The second comparison reveals that only with the reference 700 nm, the microsphere's images acquired using the set of the thirteen wavelengths present in average more reduced shadow (**Figure 2(b)**). These two types of



(a)



(b)

Figure 2. (a) Shadow size of each contrasted image corresponding to a reference wavelength, a contrasted image is an image acquired with a wavelength (light) used to fix the focal plan of the microscope, this wavelength is called reference wavelength; (b) Shadow size average over each set of the thirteen images, each set corresponds to a reference wavelength.

comparison allow to select 700 nm as the best reference wavelength to fix the focal plan of the multi spectral microscope.

3.2. Spectra Extraction and Correction Coefficients

The images acquired from different filters (filter 1, filter 2 and filter 3) with the microscope led to the extraction of their spectra in transmission and reflection modes. **Figure 3** and **Figure 4** present a comparison of these spectra

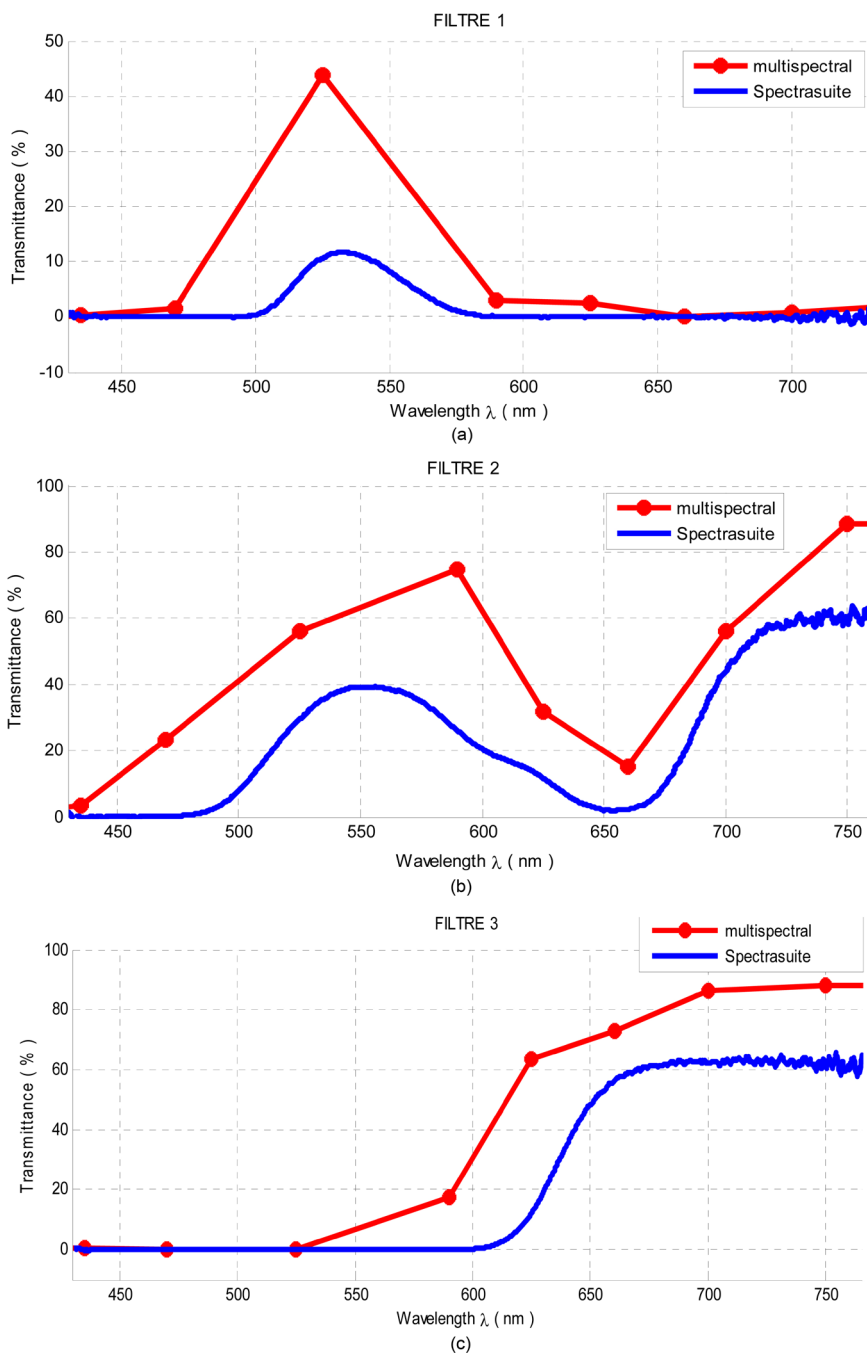


Figure 3. Transmittance Spectra for filter 1 (a), for filter 2 (b), for filter 3 (c), extracted by the standard spectrometer Spectra Suite (spectra in blue colour) and by the multi spectral microscope (spectra in red colour).

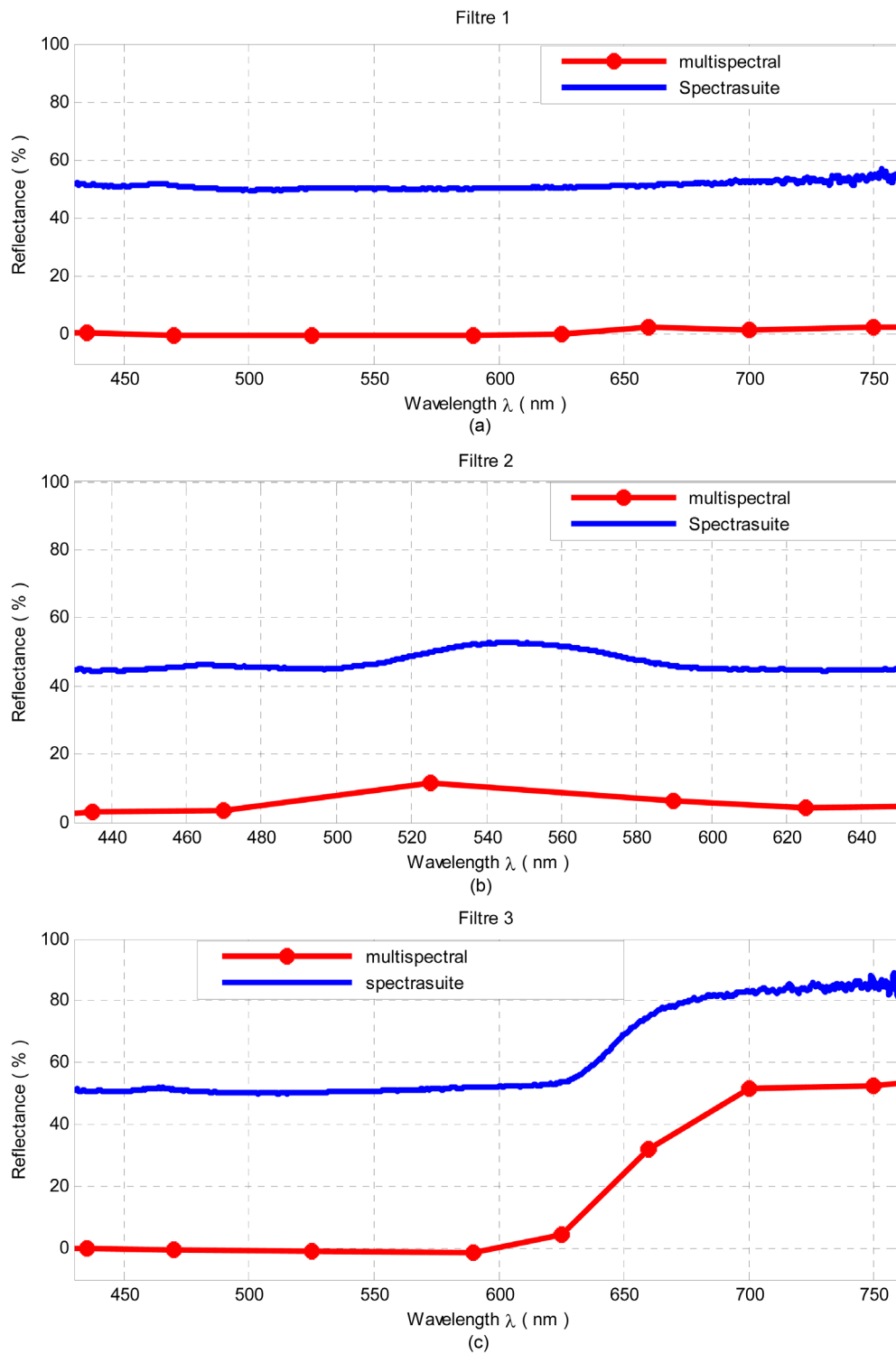


Figure 4. Reflectance Spectra for filter 1 (a), for filter 2 (b), for filter 3 (c), extracted by the standard spectrometer Spectra Suite (spectra in blue colour) and by the multi spectral microscope (spectra in red colour).

with the spectra obtained from the same filters with the spectrometer Compact Spectra Suite. We can see in **Figure 3** and **Figure 4** that in transmission mode and in reflection mode, the two types of spectra show similar

profile which indicates the nature of the different filters (filters 1, 2 and 3 are respectively pass-band, pass-band and pass-high, pass-high) but do not coincide. The filters transmit more and reflect less light than in the case we use the multi spectral microscope. So, we need to suggest a correction and make spectra in well agreement. The pixel intensity I_p from a spectral channel (p) is the contribution of the source of illumination $E_p(\lambda)$, the spectral sensibility $S(\lambda)$ of camera and the standard spectrum $f(\lambda)$ of the specimen. The intensity I_p , in absence of fluorescence is given by the Equation (4) [2] [11]:

$$I_p = \int_0^{\infty} E_p(\lambda) f(\lambda) S(\lambda) d\lambda. \quad (4)$$

The thirteen wavelengths ranging from 375 nm to 940 nm give thirteen spectral channels (p). λ takes the different values of emission spectral band of the LED. The spectra are discrete because they are built on thirteen points joint through Matlab. The points represent intensity I_p of a pixel in function of the positions of the picks for the spectral emission of the LEDs. The intensity I_p in a pixel is an average taken over an emission spectral band of a quasi-monochromatic LED source. This causes a discrepancy between the spectra obtained from the multi spectral microscope and the standard spectra [12].

The transfer function $T_p(\lambda)$ of system in each spectral channel is derived from the formula (4) [12]:

$$T_p(\lambda) = \tau_p E_p(\lambda) S(\lambda). \quad (5)$$

τ_p is a constant chosen to normalize $T_p(\lambda)$ over the passband of the channel (p).

The Equation (4) does not take into account the imperfection of the optics in the multi spectral device. That induces discrepancy between the constructed spectra and the standard spectra. Chromatic aberration, eventual fluorescence of the specimen and camera shot noise also induce this discrepancy [2]. Beside these causes, the non-monochromaticity of the LEDs contributes to the discrepancy. Indeed, if Δ_p is the size of the pass band for a spectral channel (p) around which Taylor development of standard spectrum $f(\lambda)$ is made, the Equation (4) becomes [12]:

$$I_p = f(\lambda_p) + \sum_{n=1}^N \frac{f^{(n)}(\lambda_p)}{n!} \int_{\Delta_p} T_p(\lambda) (\lambda - \lambda_p)^n d\lambda. \quad (6)$$

We can see easily the contribution for the LED's non-monochromaticity to the discrepancy. **Figure 3** shows that the discrepancy tends to disappear when the standard transmittance tends toward zero value. It appears when the standard transmittance rises up. This variation reveals that the standard and multi spectral transmittances can be linked through this linear relation:

$$T_{st} = \langle \alpha_{msp}^t \rangle T_{msp}. \quad (7)$$

T_{msp} is the transmittance spectrum got from the multi spectral microscope; T_{st} is the standard transmittance spectrum; $\langle \alpha_{msp}^t \rangle$ is the standardization coefficient for transmittance got from multi spectral device. It's an average obtained over the spectral band where discrepancy exists and over the three filters.

From spectra presented in **Figure 3**, we deduced $\langle \alpha_{msp}^t \rangle = 0.3833$. The relation (7) becomes:

$$T_{st} = 0.3833 T_{msp}. \quad (8)$$

Figure 4 presents the measures of reflectance and shows that the standard and multi spectral reflectance can be linked through this relation (9).

$$R_{st} = \langle \alpha_{msp}^r \rangle R_{msp} \quad (9)$$

R_{msp} is the reflectance spectrum got from the multi spectral microscope; R_{st} is the standard reflectance spectrum; $\langle \alpha_{msp}^r \rangle$ is the standardization coefficient for reflectance got from multi spectral device. It's an average obtained over the spectral band and over the three filters (**Figure 4**). We highlight the reflectance spectra variation through the following **Table 1** which suggests the mean value $\langle \alpha_{msp}^r \rangle$ given by the relation (10):

$$\langle \alpha_{msp}^r \rangle = \begin{cases} 56.3344 & \text{if } R_{msp} \leq 1.5\% \\ 12.2114 & \text{if } 1.5\% < R_{msp} < 10\% \\ 2.7059 & \text{if } R_{msp} \geq 10\% \end{cases}. \quad (10)$$

Table 1. Reflectance spectra variation for the different filters presented in term of values allowing the determination of $\langle \alpha_{msp}^r \rangle$.

Filters	Reflectance extracted from multi spectral device	Reflectance extracted from standard spectrometer
1 and 3	Lower than 1%, 5%	Quasi-constant close to 50%
2	Included between 1%, 5% and 10%	Included between 45% and 53%
3	Higher than 10%	Included between 55% and 85%

3.3. Determination of the Modulation Transfer Function

The modulation transfer function (FTM) is an important tool allowing to quantify an image quality. It expresses the imager's capacity to transmit information from a scene in spatial frequency domain and determines its resolution. In this work, the FTM of our multi spectral imager in transmission mode is evaluated through the edge method [13]. The algorithm for the determination of the FTM consists of the following steps [14]:

- acquisition of an image of a tilted edge,
- determination of the edge spread function ESF,
- differentiation of the ESF to obtain the line spread function LSF,
- calculation of the Fourier Transform of the LSF to obtain the FTM.

For each illumination source, we evaluated the modulation transfer function following the lines and columns of the imager (Camera pixel size: $2.2 \mu\text{m} \times 2.2 \mu\text{m}$) called respectively horizontal FTM and vertical FTM (Figure 5).

The decrement of FTM for high spatial frequencies shows that our device behaves like a low-pass filter and transmits more details in low spatial frequency band. This decrement depends on the illumination wavelength used. Using the wavelength 375 nm, the decrement of the corresponding FTM (in low spatial frequency band) is the most quick but, as we use the wavelength 700 nm, the decrement of the corresponding FTM is less quick. This confirms that images acquired with 700 nm as illumination wavelength are more contrasted whereas the images acquired with 375 nm contain less detail.

3.4. Application to Organic Microspheres

After the determination of correction coefficients, the multi spectral microscope is used to make measurements on organic polymer's microspheres of diameter $\Phi = 10.2 \mu\text{m}$ with known properties (homogeneity, isotropicity and spherical geometry). The different measures are treated through multivariate analysis methods such as principal component analysis (PCA), k-means method [15]-[22].

If a sample of three objects of colors red, green and blue is illuminated using red-light, only the red object will be observed. If it is illuminated using green light, only the green object will be seen. If it's illuminated by blue light, only the blue object will be observed. So, each wavelength reveals specific information about the specimen. Figure 6(a) presents a spectral representation of microsphere's images in transmission mode for the thirteen spectral channels corresponding to the different illumination wavelengths. In Figure 6(a), we can see thirteen images which seem to be identical; it means there's a repetition of informations from a spectral channel to another. The analysis of these spectral images using PCA allows to isolate informations [15]-[18]. Applying PCA to the spectral images data (Figure 6(a)), we condense informations into new group so that they do not present any correlation between them and are ordered in terms of the percentage of variance giving more informations (Figure 6(b)). We observe that all the informations are quasi located into the first principal component (Figure 6(b)). Therefore, the PCA means that only one spectral channel or one illumination wavelength is sufficient to describe the microsphere. So, our multi spectral device confirms that the microsphere effectively is constituted of identical elements; that is to say it's well homogeneous and isotropic.

We apply K-means to an image by dividing its intensity dispatching in five clusters. This method puts the different parts of the microsphere into different clusters according to their similar spectra. We obtained the configuration in Figure 7. This figure shows that K-means method takes into account the intensity dispatching inside the microsphere by highlighting that this dispatching is not homogeneous. Indeed, parallel light rays coming on the microsphere have not the same incidence angles. So, reflections on the impact area are not the same according to Fresnel law given by the formula (11) [23]:

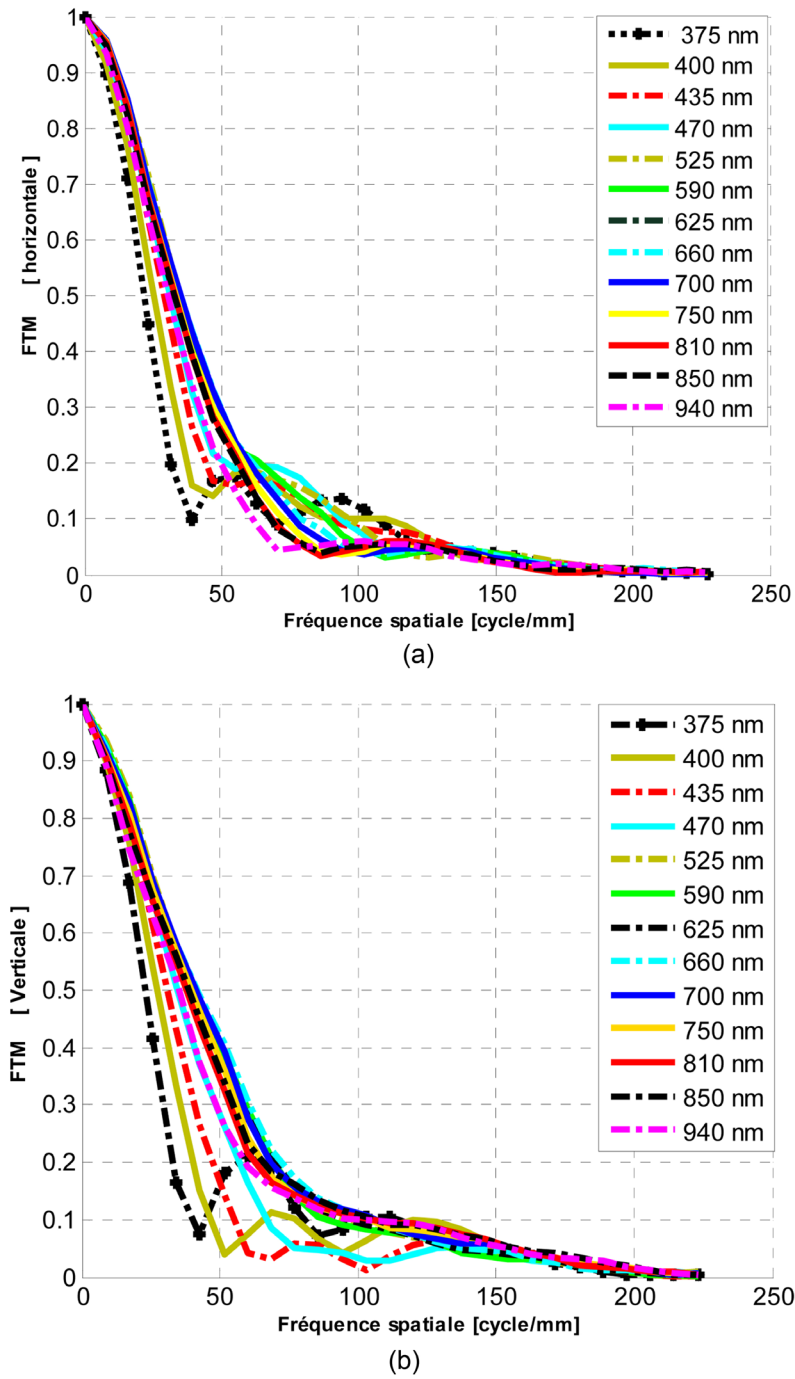


Figure 5. Modulation transfer function horizontally (a) and vertically (b) of the multi spectral imager for different quasi-monochromatic illumination sources.

$$R(\alpha_i) = 0.5 \times \left(\frac{\sin^2(\alpha_i - \alpha_r)}{\sin^2(\alpha_i + \alpha_r)} + \frac{\tan^2(\alpha_i - \alpha_r)}{\tan^2(\alpha_i + \alpha_r)} \right). \quad (11)$$

α_i and α_r are respectively incidence angle and refraction angle and R is the Reflection.

That is due to the microsphere's sphericity. Figures 8(a)-(b) present standardized spectra of a microsphere. Figure 8(c) shows a non-standardized spectrum in scattering mode.

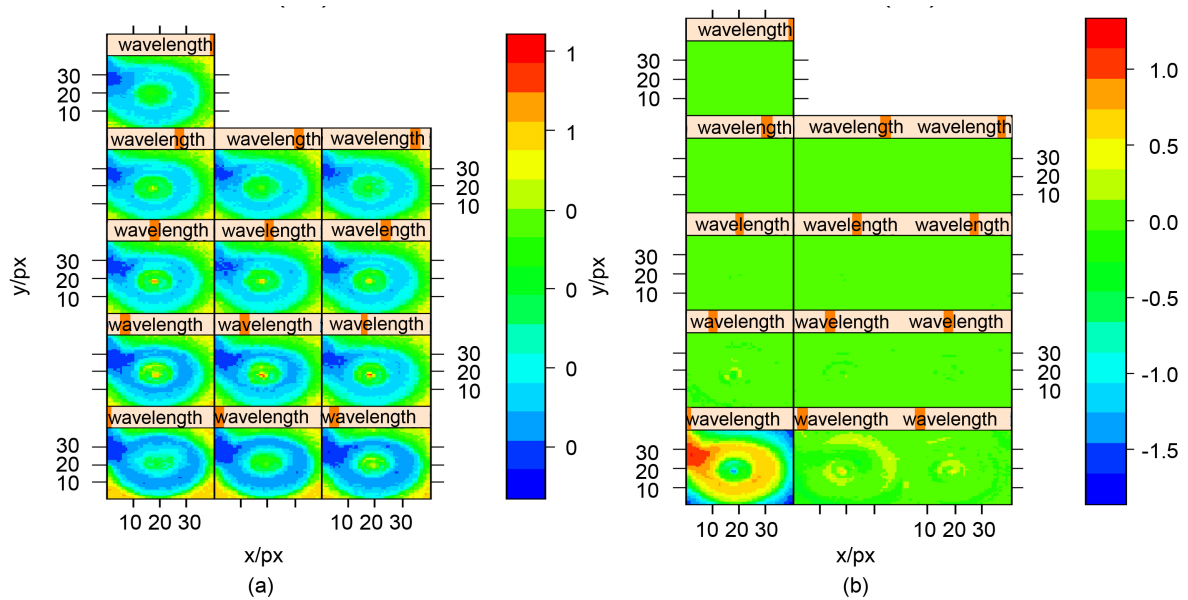


Figure 6. Spectral intensity distribution inside the microsphere in transmission mode, presented for the thirteen spectral channels (375, 400, 435, 470, 525, 590, 625, 660, 700, 750, 810, 850 and 940) in nm, starting from the bottom on the left to the top, as indicated by the orange lines (a); the new group of principal component images (PCs images) where informations are isolated using principal components analysis is presented in (b). The PCs images start by PC1 on the bottom on the left to the top as indicated by the orange lines.

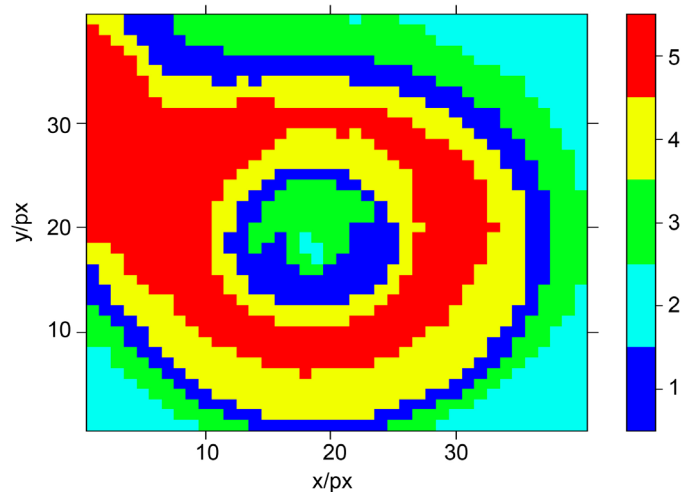


Figure 7. Intensity dispatching in the microsphere image presented by k-means method.

4. Conclusion

A low cost multi mode multi spectral microscope using a camera and a set of monochromatic Light Emitting Diodes (LEDs) ranging from 375 nm to 940 nm as illumination sources was built. The microscope allows the automated acquisition of thirteen images from the same scene of a sample illuminated by each source, and the extraction of spectra corresponding to its three modes transmission, reflection and scattering. The goal of this work is to characterize it and valid its use. So, in transmission mode we determined its modulation transfer function which is an important characteristic tool of an imager. The wavelength 700 nm was chosen to be the reference for the image acquisition. At this wavelength, the acquired images are well contrasted and diffraction effects and chromatic aberration are reduced. Measurements made with filters suggested correction coefficients in transmission mode and reflection mode. By applying PCA to the microsphere's images, the multi spectral device

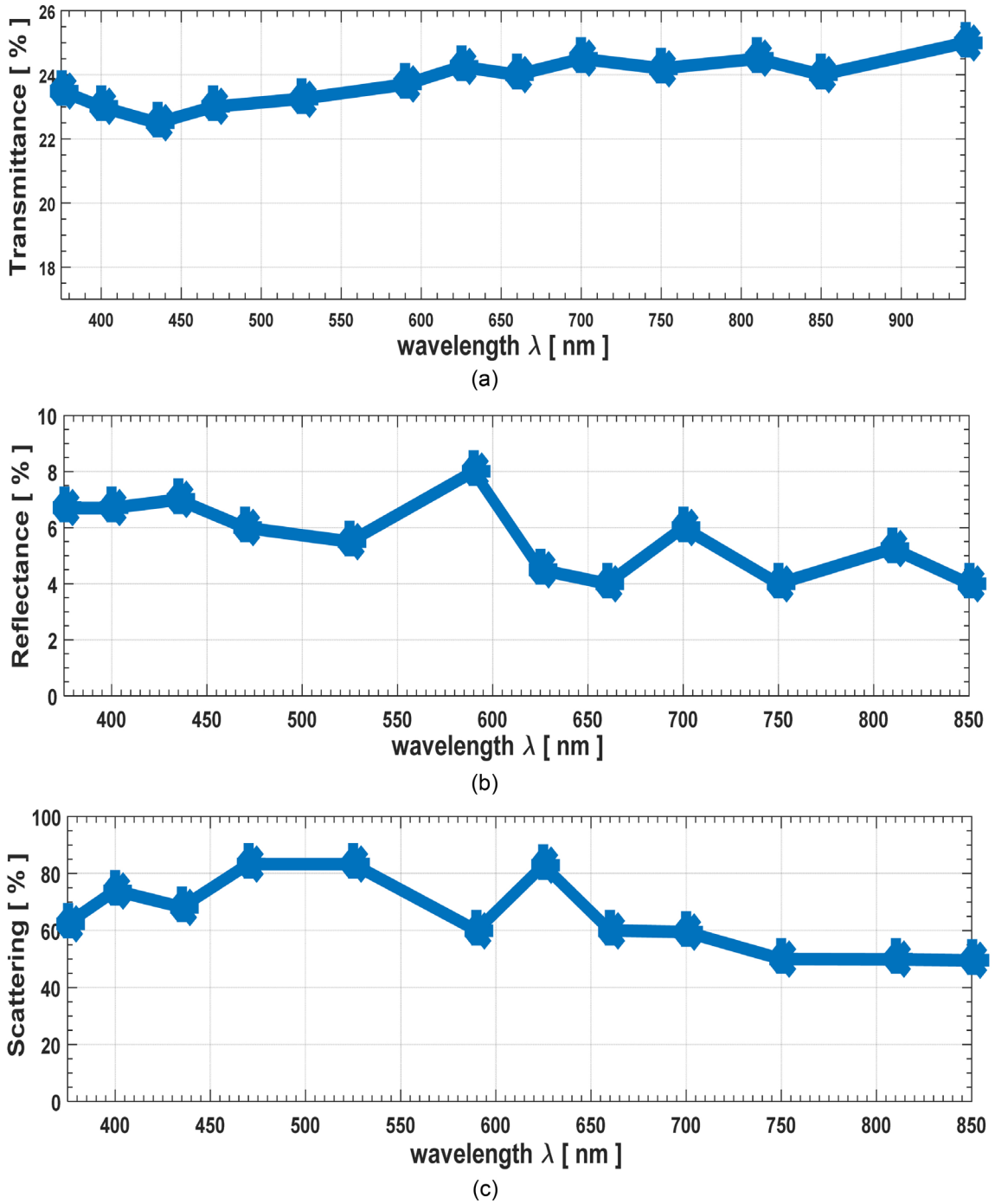


Figure 8. Standardized spectrum in transmission mode (a), standardized spectrum in reflection mode (b) and non-standardized spectrum in scattering mode (c), extracted from microsphere by the multi-spectral microscope.

has confirmed its homogeneity. Through K-means method, the experimental instrument recognized the sphericity of the microsphere. This led to the extraction of the standard transmittance and reflectance spectra. Therefore, this microscope is used as a routine instrument.

References

- [1] Zoueu, J.T., Loum, G.L., Cisse Haba, T., Brydegaard, M. and Menan, H. (2008) Optical Microscope Base on Multis-

- pectral Imaging Applied to Plasmodium Diagnosis. *Journal of Applied Sciences*, **8**, 2711-2717. <http://dx.doi.org/10.3923/jas.2008.2711.2717>
- [2] Brydegaard, M., Guan, Z. and Samberg, S. (2009) Broad-Band Multi-Spectral Microscope for imaging Transmission Spectroscopy Employing an Array of Light-Emitting Diodes (LEDs). *American Journal of Physics*, **77**, 104-110. <http://dx.doi.org/10.1119/1.3027270>
- [3] Sangare, M., Tekete, C., Bagui, O.K., Ba, A. and Zoueu, J.T. (2015) Identification of Bacterial Diseases in Rice Plants Leaves by the Use of Spectroscopic Imaging. *Applied Physics Research*, **7**, 61-69. <http://dx.doi.org/10.5539/apr.v7n6p61>
- [4] Sangare, M., Agneroh, T.A., Bagui, O.K., Traore, I., Ba, A. and Zoueu, J.T. (2015) Classification of African Mosaic Virus Infected Cassava Leaves by the Use of Multi-Spectral Imaging. *Optics and Photonics Journal*, **5**, 261-272. <http://dx.doi.org/10.4236/opj.2015.58025>
- [5] Levenson, R. and Mansfield, J. (2006) Multispectral Imaging in Biology and Medicine: Slices of Life. *Cytometry Part A*, **69A**, 748-758. <http://dx.doi.org/10.1002/cyto.a.20319>
- [6] Merdasa, A., Brydegaard, M., Svanberg, S. and Zoueu, J.T. (2013) Staining-Free Malaria Diagnostics by Multispectral and Multimodality Light-Emitting-Diode Microscopy. *Journal of Biomedical Optics*, **18**, Article ID: 036002.
- [7] Zoueu, T. and Tokou, S. (2012) Trophozoite Stage Infected Erythrocyte Contents Analysis by Use of Spectral Imaging LED Microscope. *Journal of Microscopy*, **245**, 90-99. <http://dx.doi.org/10.1111/j.1365-2818.2011.03548.x>
- [8] Strojnik, M., Wang, Y., Randolph, J.E. and Ayon, J.A. (1991) Site-Certification Imaging Sensor for the Exploration of Mars. *Optical Engineering*, **30**, 590-597. <http://dx.doi.org/10.1117/12.55842>
- [9] Strojnik, M., Wang, Y. and Paez, G. (1995) Design of a High-Resolution Telescope for an Imaging Sensor to Characterize a (Martian) Landing Site. *Optical Engineering*, **34**, 3222-3228
- [10] Rueda, L. (2014) Microarray Image and Data Analysis Theory and Practice. Electrical Engineering/Computer Science, 301-303.
- [11] Ohta, N. (1981) Maximum Errors in Estimating Spectral-Reflectance Curves from Multispectral Image Data. *Journal of the Optical Society of America*, **71**, 910-913. <http://dx.doi.org/10.1364/JOSA.71.000910>
- [12] Stephen, K. and Friedrich, O. (1977) Estimation of Spectral Reflectance Curves from Multispectral Image Data. *Applied Optics*, **12**, 3107-3114.
- [13] Estribeau, M. (2004) Analyse et modélisation de la fonction de transfert de modulation des capteurs d'images à pixels actifs CMOS, Thèse de Doctorat, Ecole Nationale Supérieure de l'Aéronautique et de l'Espace.
- [14] Egbert, B., Susanne, G. and Ulrich, N. (2003) Simple Method for Modulation Transfer Function Determination of Digital Imaging Detectors from Edge Images. *Proceedings of SPIE*, **5030**, 877-884. <http://dx.doi.org/10.1117/12.479990>
- [15] Urska, D., Paul, H., Chris, B., Stewart, A. and Sean, M. (2011) Principal Component Analysis on Spatial Data: An Overview. *Annals of the Association of American Geographers*, **103**, 1-23.
- [16] Barry, M. and Paul, G. A Brief Introduction to Multivariate Image Analysis (MIA). http://www.eigenvector.com/Docs/MIA_Intro.pdf
- [17] Besse, P.C. (1992) PCA Stability and Choice of Dimensionality. *Statistics & Probability Letters*, **13**, 405-410. [http://dx.doi.org/10.1016/0167-7152\(92\)90115-L](http://dx.doi.org/10.1016/0167-7152(92)90115-L)
- [18] Analyse en composantes Principales. http://fr.wikipedia.org/wiki/Analyse_en_composantes_principales
- [19] Shlens, J. (2014) A Tutorial on Principal Component Analysis.
- [20] Eric, W. (2014) K-Means Clustering Algorithm from Wolfram Mathworld.
- [21] DUNOD. Statistique exploratoire multidimensionnelle. 3^e Edition, 155-158.
- [22] Bloch, I. (2003) Classification et reconnaissance des formes. 17.
- [23] Chicea, D. and Turcu, I. (2005) A Random Walk Montecarl Approach to Simulate Multiple Light Scattering on Biological Suspensions. *Romanian Report in Physics*, **3**, 418-425.



Submit or recommend next manuscript to SCIRP and we will provide best service for you:

Accepting pre-submission inquiries through Email, Facebook, LinkedIn, Twitter, etc.

A wide selection of journals (inclusive of 9 subjects, more than 200 journals)

Providing 24-hour high-quality service

User-friendly online submission system

Fair and swift peer-review system

Efficient typesetting and proofreading procedure

Display of the result of downloads and visits, as well as the number of cited articles

Maximum dissemination of your research work

Submit your manuscript at: <http://papersubmission.scirp.org/>